THE JOURNAL OF PHYSICAL CHEMISTRY B LETTERS

2006, *110,* 8910−8913
Published on Web 04/18/2006

Sequence Dependence of Charge Transport Properties of DNA

C. Nogues,[†] S. R. Cohen,[‡] S. Daube,[‡] N. Apter,[‡] and R. Naaman*[,†]

Department of Chemical Physics, and Chemical Research Support, Weizmann Institute, Rehovot, 76100, Israel

Received: February 10, 2006; In Final Form: March 21, 2006

The electrical conduction through three short oligomers (26 base pairs, 8 nm long) with differing numbers of GC base pairs was measured. One strand is poly(A)−poly(T), which is entirely devoid of GC base pairs. Of the two additional strands, one contains 8 and the other 14 GC base pairs. The oligomers were adsorbed on a gold substrate on one side and to a gold nanoparticle on the other side. Conducting atomic force microscope was used for obtaining the current versus voltage curves. We found that in all cases the DNA behaves as a wide band-gap semiconductor, with width depending on the number of GC base pairs. As this number increases, the band-gap narrows. For applied voltages exceeding the band-gap, the current density rises dramatically. The rise becomes sharper with increasing number of GC base pairs, reaching more than 1 nA/nm^2 for the oligomer containing 14 GC pairs.

Control and measurement of charge transport along a molecular chain is both of fundamental interest and relevant to futuristic technologies such as molecular electronics. Due to its unique assembly and recognition properties, DNA has been widely studied in this context, and numerous works have been devoted to the characterization of the charge transport in DNA.[1−15] Consequently, some aspects of the mechanisms of charge transfer in DNA have been established. DNA-mediated charge transport can occur on an ultrafast time scale,[16,17] over distances smaller than 40 nm.[18] The lower ionization potential of guanine (G) and cytosine (C) bases, relative to the thymine (T)−adenine (A) base pairs, implicates the former in efficient current flow.[14,19] Therefore, the potential exists to control current through a DNA chain by choice of base pair sequence. A detailed description of this possibility, in terms of superexchange and hopping between GC base pairs, has been proposed.[20−23] However, experimental measurements of conductivity are complicated by the delicate and complex structure of DNA and the effect of the electrical contact between the molecule(s) and the electrodes on the observed results.[24,25]

We have previously presented an original protocol for accurately probing the current flow through short DNA strands.[11,13,26] In this protocol DNA monolayers with appropriate packing density are formed and characterized on a gold electrode, after which conducting atomic force microscopy (cAFM) is applied to probe their electrical properties. The procedure involves three key features.[11] (1) Formation of a well-defined electrical contact to the double strand DNA (dsDNA) on both ends by chemical binding to a gold electrode on one end and a 10 nm diameter gold nanoparticle (GNP) on the other (see Figure 1). (2) Embedding these Au−dsDNA−Au structures in a nonconducting monolayer of single strand DNA (ssDNA) by hybridizing the GNP-modified single strand with its complementary single strand chemisorbed on the surface electrode. This ensures that the dsDNA extends away from the surface, avoiding direct interactions of the double strand with the metallic surface which can distort the DNA conformation and perturb the conductive channel.[15,27] (3) Location of the protruding GNP using nondestructive semicontact mode AFM imaging, then passing gently and seamlessly into contact mode for the *I*/*V* measurement, as explained below and in ref 11, to preserve the integrity of the structure. The electrical measurements were recorded in air under ambient conditions of 55% relative humidity. Some experiments were performed in a controlled humidity of 10%, which did not lead to any noticeable difference in the results. Therefore ionic current is unlikely to be responsible for the current measured.[11]

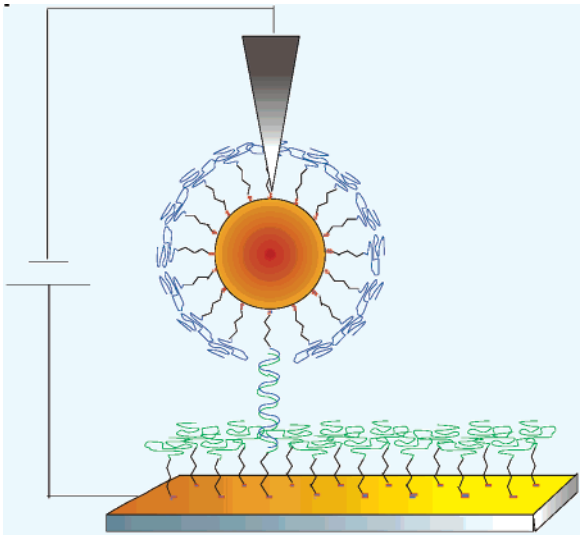

Figure 1. Schematic of a single-strand DNA (ssDNA) monolayer on gold electrode and the double-strand DNA (dsDNA) bridge between the gold substrate and the gold nanoparticle (GNP) formed through hybridization. (Reprinted with permission from ref 11.)

* Corresponding author: email: ron.naaman@weizmann.ac.il. Tel: +972-8-9342367. Fax: +972-8-9344123.
[†] Department of Chemical Physics.
[‡] Chemical Research Support.

10.1021/jp060870o CCC: $33.50

TABLE 1: DNA Sequences

GC content	sequence
0	5′-AAA AAA AAA AAA AAA AAA AAA AAA AA-3′
	3′-TTT TTT TTT TTT TTT TTT TTT TTT TT-5′
8	5′-CAT TAA TGC TAT GCA GAA AAT CTT AG-3′ (*4G*)
	3′-GTA ATT ACG ATA CGT CTT TTA GAA TC-5′ (*4G*)
14	5′-GCT GGA TGG TAT GGA GAA GAT GTG CG-3′ (*12G*)
	3′-CGA CCT ACC ATA CCT CTT CTA CAC GC-5′ (*2G*)

Using this protocol we demonstrated that a 26 base pair DNA of a sequence containing 8 GC base pairs randomly distributed along the strand can transport charges above a voltage threshold of ~1.5 V.[11,13] Here we extend this method to examine the influence of the base-pair sequence on the charge transfer in DNA. The results support the propositions regarding the enhancement due to GC pairs, and extend recent measurements made in solution.[12] Reliable measurements of DNA strands under ambient (air) conditions are critical in promoting DNA-based electronic devices. Further, the results provide insights on the relation between the electronic properties of DNA in solution and in ambient.

Three short oligomers (26 base pairs, 8 nm long) with differing numbers of GC base pairs were synthesized (See Table 1). One set of strands is poly(A)−poly(T), which is entirely devoid of GC base pairs. Of the two additional sets of strands, one contains 8 and the other 14 GC base pairs.

The 3′ end of each single strand DNA was modified with mercapto-propane ($-CH_2-CH_2-CH_2-SH$) to allow strong binding of the DNA to the gold electrodes. This short linker essentially represents a three-carbon alkanethiol through which tunneling is facile.[28,29] The current behavior should therefore be a characteristic only of the attached DNA double strand. The sample preparation for all three ssDNA monolayers is identical and follows the same procedure described previously.[11] The choice of which complementary strand was initially bound to the surface as an initial monolayer (ssDNA) and which was linked to the GNP was governed by the necessity for the layer to be insulating and relatively densely packed. Results on the monolayer density using radioactive methods[11] showed that all the ssDNA except poly(A) formed densely packed monolayers with comparable density of $2 \pm 0.5\ 10^{12}$ probes/cm^2. Poly(A) formed a much looser monolayer at $9.7 \pm 0.4\ 10^{11}$ probes/cm^2. Therefore, poly(T) was adsorbed on the flat gold surface and the poly(A) on the gold nanoparticle. For the 14 GC DNA, a monolayer composed of the G-rich single strand (containing 12 Gs) was not insulating, presumably due to the fact that guanines behave like a hole trap[21−23] and facilitate charge hopping. Therefore, this G-rich ssDNA was adsorbed on the GNP while its complementary (12 C) strand was adsorbed on the flat gold substrate to form an insulating monolayer.

The adsorption of ssDNA to GNPs was performed as previously described, with the exception of the poly(A). This oligomer exhibited low surface density (see the radioactive results in the above paragraph), and under the buffer conditions required for hybridization the GNP flocculates. To increase the poly(A) density on the GNP, the oligomer concentration in the solution was increased by 2 orders of magnitude relative to the GNP concentration. In addition, the incubation time for the monolayer formation was 20 h instead of 12 h, and following the incubation, buffer was added to the ssDNA-modified GNP solution so that the final salt concentration (NaCl) reached 0.2 M. Then the mixture was incubated for 8 h before rinsing with buffer at 0.4 M, employing a centrifugation cycle at 10 000 rcf. The ssDNA-modified GNP solutions could be kept at 4 °C for months.

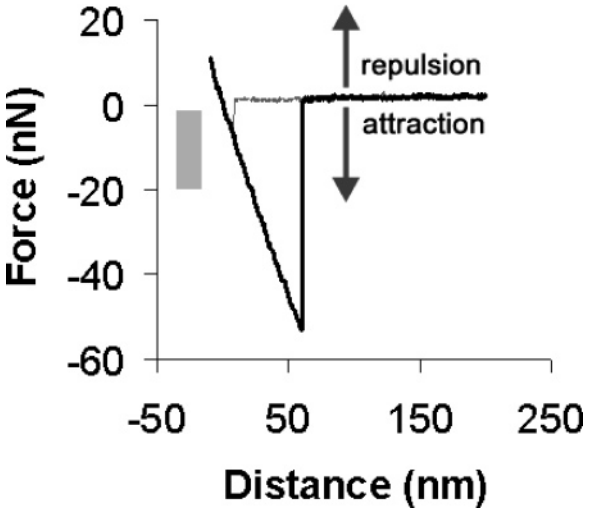

Figure 2. Typical force vs tip−sample distance curve showing both approach (light) and retracting (bold) directions. Downward deflections of approach and retraction curves are due to "snap-in" and adhesion, respectively. Net repulsive and attractive force regimes are indicated by arrows. For the *I*/*V* curves, the force was maintained at a net attractive force, as indicated by the shaded box to left of curve.

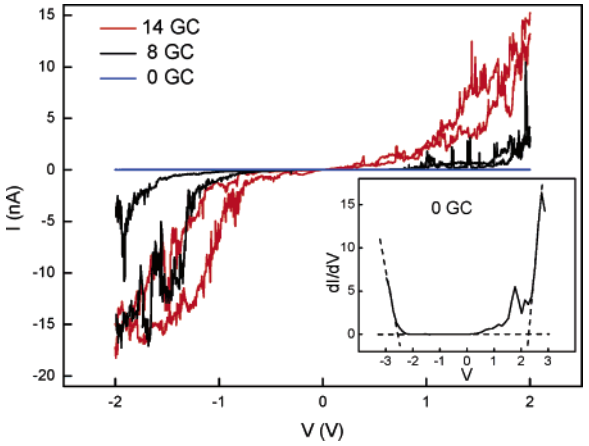

Figure 3. *I*−*V* curve characteristics for the Au-dsDNA-GNP bridge measured on three ds DNA assemblies of differing GC content: 0, 8, and 14. Inset: an example of a d*I*/d*V* versus applied voltage curve for the 0 GC base pair oligomer. The intersection of the vertical dotted lines at the *x*-axis give the value of V_T.

In the present experiments, precise vertical and lateral positioning of the AFM probe tip was controlled by a software script both to ensure accurate lateral placement and to guarantee that the same (low) force existed between tip and GNP for all the measurements. This script located the GNP within a chosen region, switched from semicontact to contact mode while controlling the force at a value representing a slight bend of the cantilever toward the surface (in the attractive region, Figure 2). The entire procedure is completed within 2−3 s so that the tip could not drift off the GNP. As a result, better reproducibility was achieved allowing a fair comparison between the different sequences.

The *I*−*V* curves display significant differences between the three samples (Figure 3). The general shape of the *I*−*V* curves is reproducible for all the sequences. The current shows a flat region at low bias, and rises above a voltage threshold V_T that increases with decreasing GC content. The inset of Figure 3 shows, as an example, the d*I*/d*V* vs V curve. obtained numerically from the *I*−*V* curve, for the sequence containing no GC pairs. The information on the band-gap, shown in Table 2, was obtained using this type of curve for all sequences studied.

TABLE 2: Voltage Threshold V_T as a Function of the GC Content and Resistance below (R_L) and above (R_H) Bias Voltage $|V| = 1$

GC content	voltage threshold (mean ± SD, $n = 40$)	R_L (at $\|V\| < 1V$) GΩ	R_H (at $\|V\| > 1V$) tGΩ
0	2.6 ± 0.09 V	1800 ± 244	686 ± 190
8	1.9 ± 0.10 V	770 ± 211	69 ± 47
14	0.9 ± 0.12 V	37 ± 15.	0.53 ± 0.2

TABLE 3: Current Density at 1.5 V as a Function of the GC Content

GC content	current density (mean ± SE, $n = 40$)
0	0.02 ± 0.01 nA/nm^2
8	0.18 ± 0.05 nA/nm^2
14	1.72 ± 0.29 nA/nm^2

For each DNA sequence, at least 40 $I-V$ curves similar to those shown in Figure 3 were accumulated, using several different conducting tips. Average resistance values at low $|V| < 1$ V (R_L) and high $|V| > 1$ V (R_H) bias regimes were thus observed. Both V_T and the measured resistance values show clear trends with increasing GC content (see Table 2). For the poly(A)−poly(T), R_L is only twice as large as for the 8 GC base pair content strands, while for the 14 GC content R_L drops by more than an order of magnitude. Above a bias of 1 V, the resistance measured, R_H drops by an order of magnitude between the 0 GC and 8 GC strands, and again by another 2 orders of magnitude for the 14 GC strands (686±190 GΩ for the 0 GC, 69±47 GΩ for the 8 GC, and 0.53±0.2 GΩ for the 14 GC). In addition, the value of the voltage threshold from which the current increases depends strongly on the sequence, as it occurs at progressively lower bias for the oligomers containing more GC pairs (Table 2). V_T, the voltage threshold, corresponds to the intersection of the two fitted lines following the high and low bias regimes on the corresponding differential resistance dI/dV vs V curves (see inset Figure 3).

The calculated values of the current density measured at 1.5 V are shown in Table 3. From geometric considerations, there can be up to 3 dsDNAs of 2 nm diameter and 8 nm length bridging the two electrodes.[11] Maximum resistance per chain would be calculated when only one dsDNA bridge carries all the current. The reported values here relate to this maximum. Hence, the lower limit for the current density is one-third of the values reported in Table 3. The values of the current density at 1.5 V are measured on curves smoothed by five-point adjacent averaging. The current density increases by an order of magnitude for each increment in GC content studied (Table 3). However, at the high bias region, as mentioned above, the difference in resistance between 8 GC and 14 GC is 2 orders of magnitude. It is significant that the standard error increases with the GC content, as it reflects the stability of current response. This is particularly evident at the higher biases used: for voltage sweeps larger than 2 V (from 1.5 to +1.5 V), these fluctuations increase significantly for the strands with highest GC content.

The approach used here has allowed us to investigate the influence that the DNA base sequence has on its charge transfer properties. The GC DNA content appears to strongly influence the electrical properties of DNA. The DNA behaves as a broad band-gap semiconductor, whose band gap energy decreases with increasing number of GC bases. This role of the GC base pair has been observed before and was rationalized based on the fact that guanine has the lowest electrochemical potential of all bases,[19] and therefore was found to facilitate charge transfer along the DNA. However, the results presented here show that, in addition to lowering of the gap, the GC pairs lower the resistance, so that the current density increases with the GC base pair content. The increase in current density is evident over the entire bias range. Our findings can be compared to recently published work by Xu et al.[12] and Iqbal et al.[14] where it has been found that the current rises steadily with GC content of the DNA strand. Although the experiments were performed in very different conditions (liquid versus ambient and DNA vertical versus lying flat on a substrate), our results are consistent with those reported measurements. The current density observed in the present study, as well as in other recent works,[11−14] is not consistent with the "hopping" mechanism usually associated with charge transfer through long DNA strands, since the current density observed is too high.[30] Hence, we must conclude that the conduction observed here is through a coherent process. This means that the "band gap" observed does not necessarily reflect the total density of electronic states, but rather density of delocalized states, namely states through which charge can be transported coherently through the whole strand.

In summary, the present investigation expands our understanding of conduction through DNA, demonstrates again the importance of the GC base pair for the conduction, but indicates also that there is a very efficient and coherent conduction mechanism that allows transport of high current densities through 26 base pairs.

Acknowledgment. We acknowledge support of the G.M.J. Schmidt Minerva Center of Supramolecular Architectures and the James Franck Foundation.

References and Notes

(1) Fink, H. W.; Schonenberger, C. *Nature* **1999**, *398*, 407.
(2) Cai, L. T.; Tabata, H.; Kawai, T. *Appl. Phys. Lett.* **2000**, *77*, 3105.
(3) de Pablo, P. J.; Moreno-Herrero, F.; Colchero, J.; Herrero, J. G.; Herrero, P.; Baro, A. M.; Ordejon, P.; Soler, J. M.; Artacho, E. *Phys. Rev. Lett.* **2000**, *85*, 4992.
(4) Porath, D.; Bezryadin, A.; de Vries, S.; Dekker, C. *Nature* **2000**, *403*, 635.
(5) Kasumov, A. Y.; Kociak, M.; Gueron, S.; Reulet, B.; Volkov, V. T.; Klinov, D. V.; Bouchiat, H. *Science* **2001**, *291*, 280.
(6) Storm, A. J.; van Noort, J.; de Vries, S.; Dekker, C. *Appl. Phys. Lett.* **2001**, *79*, 3881.
(7) Watanabe, H.; Manabe, C.; Shigematsu, T.; Shimotani, K.; Shimizu, M. *Appl. Phys. Lett.* **2001**, *79*, 2462.
(8) Yoo, K. H.; Ha, D. H.; Lee, J. O.; Park, J. W.; Kim, J.; Kim, J. J.; Lee, H. Y.; Kawai, T.; Choi, H. Y. *Phys. Rev. Lett.* **2001**, *8719*, 198102.
(9) Zhang, Y.; Austin, R. H.; Kraeft, J.; Cox, E. C.; Ong, N. P. *Phys. Rev. Lett.* **2002**, *89*, 198102.
(10) Heim, T.; Deresmes, D.; Vuillaume, D. *J. Appl. Phys.* **2004**, *96*, 2927.
(11) Nogues, C.; Cohen, S. R.; Daube, S. S.; Naaman, R. *Phys. Chem. Chem. Phys.* **2004**, *6*, 4459.
(12) Xu, B. Q.; Zhang, P. M.; Li, X. L.; Tao, N. J. *Nano Lett.* **2004**, *4*, 1105.
(13) Cohen, H.; Nogues, C.; Naaman, R.; Porath, D. *Proc. Natl. Acad. Sci. U.S.A.* **2005**, *102*, 11589.
(14) Iqbal, S. M.; Balasundaram, G.; Ghosh, S.; Bergstrom, D. E.; Bashir, R. *Appl. Phys. Lett.* **2005**, *86*, 153901.
(15) Xu, M. S.; Endres, R. G.; Tsukamoto, S.; Kitamura, M.; Ishida, S.; Arakawa, Y. *Small* **2005**, *1*, 1168.
(16) *Long-Range Charge Transfer in DNA II*; Springer-Verlag:Berlin, 2004; Vol. 237.
(17) *Long-Range Charge Transfer in DNA I*; Springer-Verlag:Berlin, 2004; Vol. 237.
(18) Porath, D.; Cuniberti, G.; Di Felice, R. In *Topics in Current Chemistry*; Shuster G., Ed.; Springer: Berlin, 2003; Vol. 237, p 183.
(19) Di Ventra, M.; Zwolak, M. DNA Electronics in *Encyclopedia of Nanoscience and Nanotechnology*; American Scientific Publishers: California, 2004.
(20) Jortner, J.; Bixon, M.; Langenbacher, T.; Michel-Beyerle, M. E. *Proc. Natl. Acad. Sci. U.S.A.* **1998**, *95*, 12759.
(21) Shuster, G. *Acc. Chem. Res.* **2000**, *33*, 253.
(22) Giese, B. *Acc. Chem. Res.* **2000**, *33*, 631.
(23) O'Neill, M. A.; Barton, J. K. *Top. Curr. Chem.* **2004**, *236*, 67.

(24) Cui, X. D.; Primak, A.; Zarate, X.; Tomfohr, J.; Sankey, O. F.; Moore, A. L.; Moore, T. A.; Gust, D.; Harris, G.; Lindsay, S. M. *Science* **2001**, *294*, 571.
(25) Salomon, A.; Cahen, D.; Lindsay, S.; Tomfohr, J.; Engelkes, V. B.; Frisbie, C. D. *Adv. Mater.* **2004**, *16*, 477.
(26) Cohen, H.; Nogues, C.; Ullien, D.; Daube, S.; Naaman, R.; Porath, D. *Faraday Discuss.* **2006**, *131*, 367.
(27) Kasumov, A. Y.; Klinov, D. V.; Roche, P. E.; Gueron, S.; Bouchiat, H. *Appl. Phys. Lett.* **2004**, *84*, 1007.
(28) Widrig, C. A.; Alves, C. A.; Porter, M. D. *J. Am. Chem. Soc.* **1991**, *113*, 2805.
(29) McDermott, C. A.; McDermott, M. T.; Green, J.-B.; Porter, M. D. *J. Phys. Chem.* **1995**, *99*, 13257.
(30) Bixon, M.; Jortner, J. *Adv. Chem. Phys.* **1999**, *106*, 35.